



## FT-IR, FT-Raman, NMR spectra and DFT calculations on 4-chloro-N-methylaniline

A. Usha Rani<sup>a,b</sup>, N. Sundaraganesan<sup>c,\*</sup>, M. Kurt<sup>d</sup>, M. Cinar<sup>e</sup>, M. Karabacak<sup>e</sup><sup>a</sup> Avvaiyar Government College for Women, Karaikal 609602, India<sup>b</sup> Research and Development Centre, Bharathiar University, Coimbatore 641046, India<sup>c</sup> Department of Physics (Engg.), Annamalai University, Annamalai Nagar, Chidambaram 608002, Tamil Nadu, India<sup>d</sup> Ahi Evran Üniversitesi Fen Edebiyat Fakültesi Fizik Bölümü, Aşıkpaşa Kampüsü 40100, Kırşehir, Turkey<sup>e</sup> Department of Physics, Afyonkarahisar Kocatepe University, 03040 Afyonkarahisar, Turkey

## ARTICLE INFO

## Article history:

Received 21 November 2009

Received in revised form 10 January 2010

Accepted 3 February 2010

## Keywords:

FT-IR

FT-Raman

<sup>1</sup>H NMR<sup>13</sup>C NMR

TED

4-Chloro-N-methylaniline

## ABSTRACT

In this work, the vibrational spectral analysis was carried out by using FT-IR and FT-Raman spectroscopy in the range 400–4000 and 50–3500 cm<sup>-1</sup> respectively, for the title molecule. The structural and spectroscopic data of the molecule in the ground state were calculated by using density functional method using 6-311++G(d,p) basis set. The vibrational frequencies were calculated and scaled values were compared with experimental FT-IR and FT-Raman spectra. The observed and calculated frequencies are found to be in good agreement. The complete assignments of all the vibrational mode were performed on the basis of the total energy distributions (TED). <sup>13</sup>C and <sup>1</sup>H NMR chemical shifts results were given and are in agreement with the corresponding experimental values. The theoretically constructed FT-IR and FT-Raman spectra exactly coincides with experimental one.

© 2010 Elsevier B.V. All rights reserved.

## 1. Introduction

Aromatic amines, more generally anilines have been widely used as chemical dye industries, nano-cable manufacturing in electronic industries, coating by electro-polymerization in steel industries pharmaceuticals' manufacturing and other industrial purposes [1–5]. Moreover, some derivatives of aniline are used as local anesthetics in medicine. As a result, understanding of physical properties of aniline and its derivatives is crucial. The large numbers of experimental [6–8] and theoretical investigations have focused on elucidating the structure and normal vibrations of aniline and its methyl derivatives [1–3,9–11]. The structure of aniline was reported theoretically using semi-empirical [12,13] and ab initio methods [12–15]. Vibrational analysis based on FT-IR in vapour, solution and liquid phases and Raman spectra in liquid state have been reported for aniline [16]. It was also studied in the gas phase from microwave spectroscopy [1,17] and in the solid state from X-ray crystallography [18]. Reuben investigated the isotopic multiplets in the <sup>13</sup>C NMR spectra of aniline derivatives and nucleosides with partially deuterated amino groups based on effect of intra- and intermolecular hydrogen bonding [19]. Many studies [1,9,20–22] were performed recently to assign complete vibrational mode and frequency analysis. Altun et al. also stud-

ied vibrational modes and frequency analysis of *m*-methylaniline [1]. Some band observations of *p*-methylaniline in the IR spectrum are given in the literature [6,23–26]. The vibrational spectrum of chloromethyl aniline [25] and fluoromethyl aniline [27,28] is given in the literature. Shanker et al. studied 2-chloro-6-methylaniline using polarized Raman and IR spectra [29]. Barluenga et al. synthesized 2-chloro-N-methylaniline and studied its <sup>1</sup>H and <sup>13</sup>C NMR spectra [30]. The low temperatures <sup>13</sup>C NMR spectra allowed the determination of the rotational barrier of N-methyl aniline in solution was reported by Lunazzi et al. [31]. Barr et al. published a study on <sup>1</sup>H, <sup>13</sup>C, <sup>15</sup>N, <sup>19</sup>F, <sup>29</sup>Si NMR chemical shifts and coupling constants for nine N-substituted anilines [32]. Jet-cooled Fourier-transform microwave spectrum of N-methylaniline was recorded in the region of 10–26 GHz. It is analyzed to determine rotational constants and nuclear quadruple coupling constants by Fujitake et al. [8]. They gave a brief and detailed explanation of spectral analysis. Stein et al. reported that the two-dimensional solid state NMR studies of poly(aniline) [33]. Recently we reported an experimental and theoretical study on <sup>1</sup>H, <sup>13</sup>C and DEPT NMR spectra of N1-methyl-2-chloroaniline and 2-chloro-6-methylaniline along with IR, Raman and UV spectra [34,35].

Till now a detailed analysis of vibrational frequencies, IR and Raman spectra of 4-chloro-N-methylaniline (4-CINMA) has not been reported. As a result we set out experimental and theoretical investigation of the vibrational and NMR spectra of this molecule. The density functional theory (B3LYP) calculations have been performed. We worked a detailed interpretation of the vibrational

\* Corresponding author. Tel.: +91 413 2281354.

E-mail address: [sundaraganesan.n2003@yahoo.co.in](mailto:sundaraganesan.n2003@yahoo.co.in) (N. Sundaraganesan).

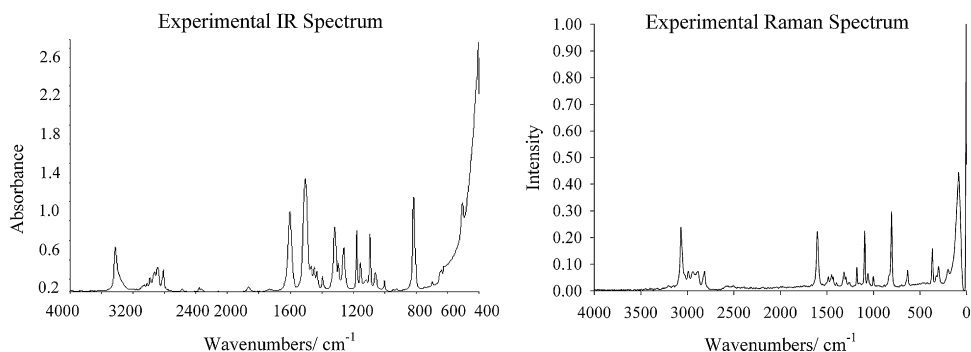


Fig. 1. The observed infrared and Raman spectra of 4-chloro-N-methylaniline.

spectra of 4-CINMA on the basis of calculated total energy distribution (TED).

## 2. Experimental

The compound 4-chloro-N-methylaniline (4-CINMA) in the solid form was purchased from Sigma–Aldrich chemical Company (U.S.A.) with a stated purity of greater than 98%, and it was used as such without further purification. The FT-Raman spectrum of 4-CINMA have been recorded using 1064 nm line of Nd:YAG laser as excitation wavelength in the region 50–3500  $\text{cm}^{-1}$  on a Bruker Model IFS 66V Spectrometer equipped with FRA 106 FT-Raman module accessory. The FT-IR spectrum of this compound was recorded in the range of 400–4000  $\text{cm}^{-1}$  on IFS 66V spectrometer using KBr pellet technique. The spectrum was recorded at room temperature with scanning speed of 10  $\text{cm}^{-1} \text{min}^{-1}$  and the spectral resolution of 2.0  $\text{cm}^{-1}$ . The observed experimental FT-IR and FT-Raman spectra along with theoretical spectra are shown in Figs. 1 and 2. The spectral measurements were carried out at the Central ElectroChemical Research Institute (CECRI) Karaikudi, Tamil Nadu, India. NMR experiments were performed in Varian Infinity Plus spectrometer at 300 K. The compound was dissolved in chloroform ( $\text{CDCl}_3$ ). Chemical shifts were reported in ppm relative to tetramethylsilane (TMS) for  $^1\text{H}$  and  $^{13}\text{C}$  NMR spectra.  $^1\text{H}$ ,  $^{13}\text{C}$  and DEPT NMR spectra were obtained at a base frequency of 75 MHz for  $^{13}\text{C}$  and 300 MHz for  $^1\text{H}$  nuclei and are shown in Figs. 3–5.

## 3. Computational details

The entire calculations were performed at density functional (DFT) level on a Pentium IV/3.02 GHz personal computer using Gaussian 03 [36] program package, invoking gradient geometry optimization [37]. The geometry of the title compound together with that of tetramethylsilane (TMS) is fully optimized.  $^1\text{H}$  and  $^{13}\text{C}$  NMR chemical shifts are calculated with GIAO approach [38] by applying B3LYP method. The theoretical  $^1\text{H}$  and  $^{13}\text{C}$  NMR chemical shifts were obtained by subtracting the GIAO calculations.  $^{13}\text{C}$  isotropic magnetic shielding (IMS) of any X carbon atoms was made according to value  $^{13}\text{C}$  IMS of TMS,  $\text{CS}_X = \text{IMS}_{\text{TMS}} - \text{IMS}_X$ . The optimized structural parameters were used in the vibrational frequency calculations at DFT level using 6-311++G(d,p) basis set to characterize all stationary points as minima. Polarization functions have been added for the better treatment of the chlorine, methyl and N–H groups. Analytic frequency calculations at the optimized geometry were done to confirm the optimized structure to be an energy minimum and to obtain theoretical vibrational spectra. The total energy distribution (TED) was calculated by using the scaled quantum mechanic (SQM) program [39] and the fundamental modes were characterized by their TED.

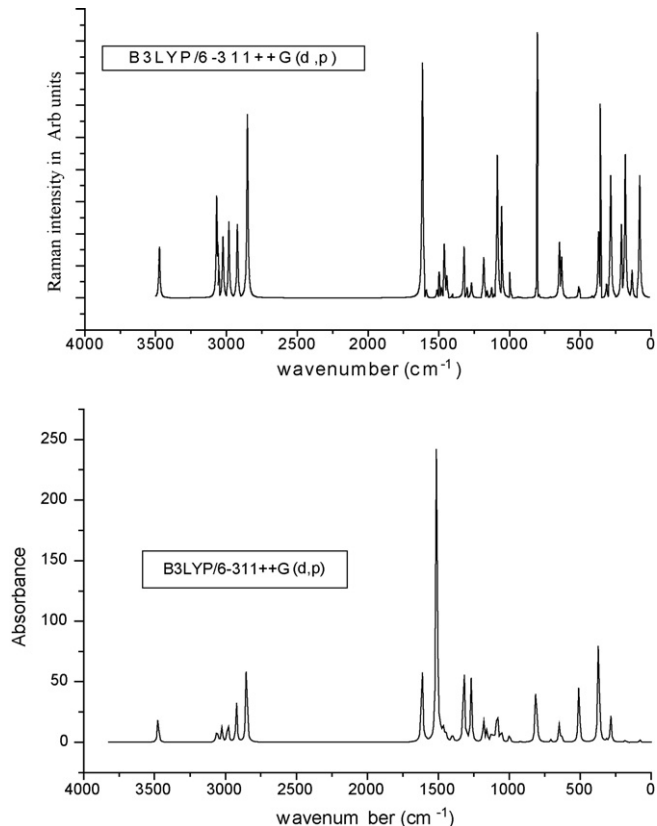


Fig. 2. The simulated Infrared and Raman spectra of 4-chloro-N-methylaniline obtained by DFT (B3LYP).

### 3.1. Prediction of Raman intensities

The Raman activities ( $S_i$ ) calculated with Gaussian 03 program [36] converted to relative Raman intensities ( $I_i$ ) using the following relationship derived from the intensity theory of Raman scattering [40,41].

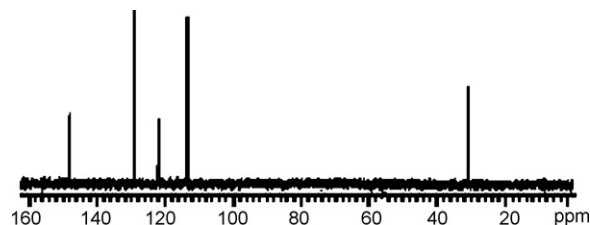


Fig. 3. The experimental  $^{13}\text{C}$  NMR spectrum of 4-chloro-N-methylaniline (in  $\text{CDCl}_3$ ).

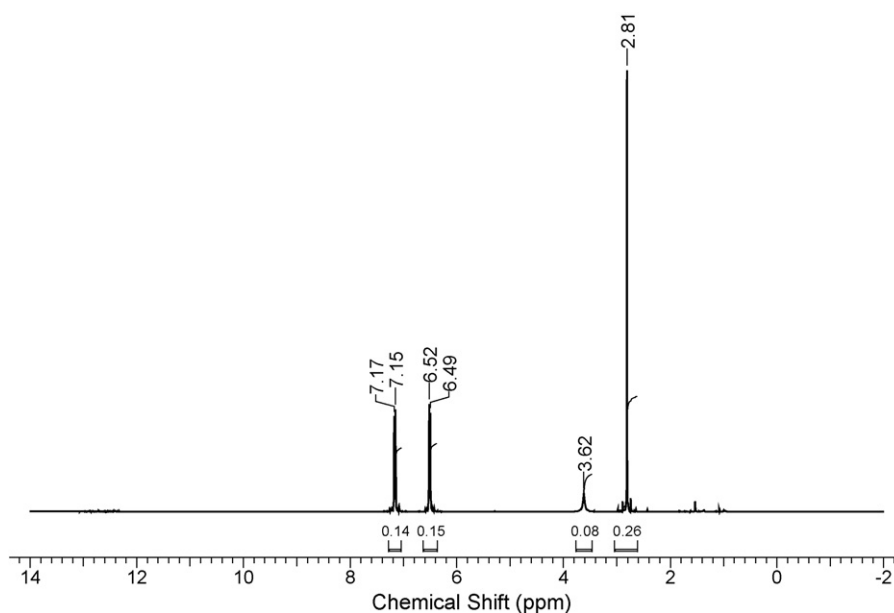


Fig. 4. The experimental  $^1\text{H}$  NMR spectrum of 4-chloro-N-methylaniline (in  $\text{CDCl}_3$ ).

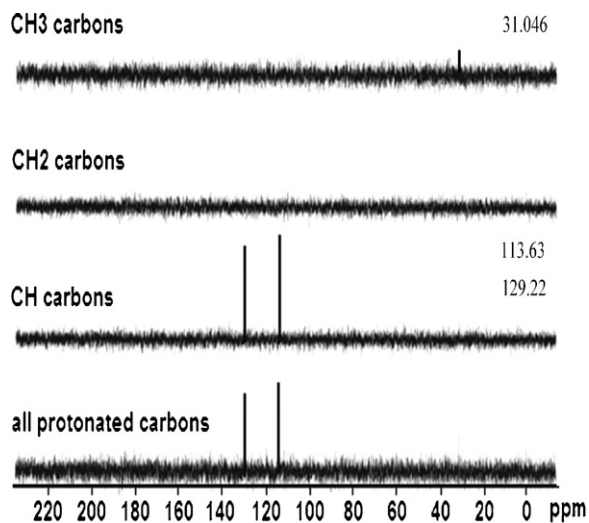


Fig. 5. The experimental DEPT NMR spectra of 4-chloro-N-methylaniline (in  $\text{CDCl}_3$ ).

$$I_i = \frac{f(\nu_o - \nu_i)^4 S_i}{\nu_i [1 - \exp(-hc\nu_i/kt)]}$$

where  $\nu_o$  is the exciting wavenumber in  $\text{cm}^{-1}$ ,  $\nu_i$  the vibrational wavenumber of the  $i$ th normal mode,  $h$ ,  $c$  and  $k$  are fundamental constants, and  $f$  is a suitably chosen common normalization factor for all peak intensities. For simulation of calculated FT-Raman spectra have been plotted using pure Lorentzian band shape with a bandwidth (FWHM) of  $10 \text{ cm}^{-1}$  as shown in Fig. 2.

## 4. Results and discussions

### 4.1. Molecular geometry

As seen in Fig. 6, the numbering of atoms for title molecule is given. The optimized geometrical bond lengths, bond angles and dihedral angles by DFT/B3LYP method with 6-311++G(d,p) as basis set are listed in Table 1. Since the crystal structure of exact title

compound is not available till now, the optimized structure can only be compared with other similar systems for which the crystal structures have been solved, for example *p*-chloroaniline and gas phase geometry of N1-methyl-2-chloroaniline [34,42]. As seen from Table 1, most of the optimized bond lengths are slightly larger and shorter than experimental values and the bond angles are

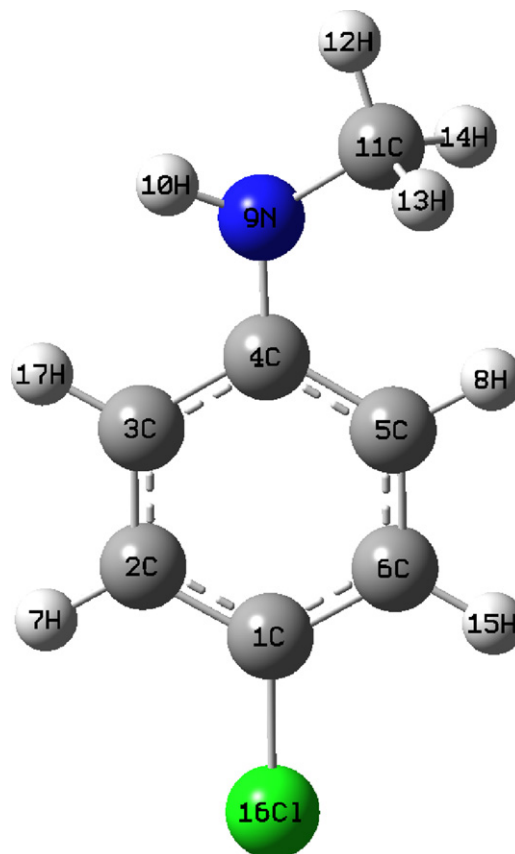


Fig. 6. The theoretical geometric structure and atom numbering of 4-chloro-N-methylaniline.

**Table 1**  
Optimized geometry of 4-chloro-N-methylaniline in ground state.

Parameters	Exp. <sup>a</sup> , XRD	Gas phase goem. <sup>b</sup>	B3LYP
<b>Bond lengths (Å)</b>			
C1–C2	1.37	1.395	1.393
C1–C6	1.37	1.392	1.388
C1–Cl16	1.41		1.763
C2–C3		1.385	1.387
C2–H7		1.083	1.083
C3–C4	1.40	1.421	1.408
C3–H17			1.086
C4–C5		1.409	1.405
C4–N9	1.40	1.376	1.388
C5–C6		1.391	1.394
C5–H8		1.082	1.082
C6–H15		1.084	1.083
N9–H10		1.007	1.008
N9–C11		1.448	1.451
C11–H12		1.090	1.090
C11–H13		1.099	1.099
C11–H14		1.095	1.094
<b>Bond angles (°)</b>			
C2–C1–C6	122.2	119.0	120.3
C2–C1–Cl16			119.7
C6–C1–Cl16	118.9		120.0
C1–C2–C3		120.0	119.7
C1–C2–H7		120.8	120.1
C3–C2–H7		119.1	120.0
C2–C3–C4		122.3	121.2
C2–C3–H17			119.3
C4–C3–H17		116.5	119.5
C3–C4–C5	118.9	121.2	118.0
C3–C4–N9		122.2	119.8
C5–C4–N9	120.6	121.2	122.2
C4–C5–C6	120.2	119.2	120.8
C4–C5–H8		119.4	120.5
C6–C5–H8		120.	118.8
C1–C6–C5	119.3	120.9	120.0
C1–C6–H15		120.0	120.1
C5–C6–H15		119.	119.9
C4–N9–H10		115.9	114.8
C4–N9–C11		123.0	122.2
H10–N9–C11		117.2	115.4
N9–C11–H12		108.4	108.6
N9–C11–H13		112.7	113.1
N9–C11–H14		111.1	110.8
H12–C11–H13		108.3	108.5
H12–C11–H14		107.6	107.5
H13–C11–H14		108.2	108.2
<b>Dihedral angles (°)</b>			
C(6)–C(1)–C(2)–C(3)			0.2
C(6)–C(1)–C(2)–H(7)			–179.8
Cl(16)–C(1)–C(2)–C(3)			–179.9
Cl(16)–C(1)–C(2)–H(7)			–0.0
C(2)–C(1)–C(6)–C(5)			0.0
C(2)–C(1)–C(6)–H(15)			179.7
Cl(16)–C(1)–C(6)–C(5)			–179.7
Cl(16)–C(1)–C(6)–H(15)			–0.0
C(1)–C(2)–C(3)–C(4)			–0.1
C(1)–C(2)–C(3)–H(17)			179.4
H(7)–C(2)–C(3)–C(4)			179.9
H(7)–C(2)–C(3)–H(17)			–0.4
C(2)–C(3)–C(4)–C(5)			–0.2
C(2)–C(3)–C(4)–N(9)		178.4	178.1
H(17)–C(3)–C(4)–C(5)			–179.7
H(17)–C(3)–C(4)–N(9)			–1.3
C(3)–C(4)–C(5)–C(6)			0.4
C(3)–C(4)–C(5)–H(8)			–179.7
N(9)–C(4)–C(5)–C(6)		–178.2	–177.8
N(9)–C(4)–C(5)–H(8)			1.9
C(3)–C(4)–N(9)–H(10)			19.2
C(3)–C(4)–N(9)–C(11)			167.5
C(5)–C(4)–N(9)–H(10)			–162.3
C(5)–C(4)–N(9)–C(11)			–14.1
C(4)–C(5)–C(6)–C(1)			–0.3
C(4)–C(5)–C(6)–H(15)			179.8
H(8)–C(5)–C(6)–C(1)			179.80
H(8)–C(5)–C(6)–H(15)			0.0
C(4)–N(9)–C(11)–H(12)			–176.1
C(4)–N(9)–C(11)–H(13)			–55.5
C(4)–N(9)–C(11)–H(14)			66.15
H(10)–N(9)–C(11)–H(12)			–27.9
H(10)–N(9)–C(11)–H(13)			92.5
H(10)–N(9)–C(11)–H(14)			–145.8

<sup>a</sup> Taken from Ref. [42].

<sup>b</sup> Taken from Refs. [34,42].

slightly different from experimental ones, because the molecular states are different during experimental and theoretical process, one isolated molecule is considered in gas phase during theoretical calculation, while many packing molecules are treated in condensed phase during the experimental measurements.

In the title molecule studied here introduction of two substituent groups on the benzene ring causes some changes in the ring C–C bond distances and also the position of the substituents in the benzene ring as well as its electron donor/acceptor capabilities plays a vital role on the structural and electronic properties of the molecules. The methyl group and chlorine atom are referred as electron-donating and electron-accepting substituents in aromatic ring systems. The carbon atoms are bonded to the hydrogen atoms with  $\sigma$  bond in benzene and substitution of a Cl and CH<sub>3</sub> groups for hydrogen reduces the electron density at the ring carbon atom. The ring carbon atoms in substituted benzenes exert a large attraction on the valence electron cloud of the hydrogen atom resulting in an increase in the C–H force constants and a decrease in the corresponding bond length. The reverse holds well on substitution with electron-donating groups. The actual change in the C–H bond length would be influenced by the combined effects of the inductive-mesomeric interaction and the electric dipole field of the polar substituent. In this study the C–H bond lengths were calculated at 1.082, 1.083, 1.083 and 1.086 Å for the ring.

As seen in Table 1, the interaction between the aminomethyl group and the aromatic ring produces a small displacement of the nitrogen atom out-of-plane of benzene ring with a torsional angle of N9–C4–C5–C6 in the ca.  $-177^\circ$ . The same trend is not exhibited in the other part of the ring because of substitution of chlorine atom as shown in Table 1 (Cl16–C1–C6–C5 =  $-179.8^\circ$ ) with an electron-donating and electron-withdrawing substituents at the para positions. The symmetry of the benzene ring is distorted, yielding ring angles smaller than  $120^\circ$  and slightly larger than  $120^\circ$  at the point of substitution. Similar values are found to be present in other aniline derivatives which are *m*-methylaniline [26], *o*-methylaniline [11] and *p*-methylaniline [6]. The C4–N9 bond distance of ca. 1.388 Å is just 0.042 Å lower than the reported experimental value of 1.43 Å for *p*-methylaniline [3].

#### 4.2. Vibrational spectral analysis

Vibrational spectral assignments have been performed on the recorded FT-IR and FT-Raman spectra based on theoretically predicted wavenumbers by density functional (B3LYP) method using 6-311++G(d,p) basis set have been collected in Table 2. On the basis of a C<sub>s</sub> symmetry the 45 fundamental vibrations of 4-CINMA can be distributed as 31A' + 14A''. The vibrations of the A' species are in-plane and those of the A'' species are out-of-plane. If we take into account the C<sub>s</sub> symmetry of this molecule, there are two imaginary frequencies correspond to N–CH<sub>3</sub> out-of-plane bending and methyl rotation perpendicular to the ring plane. The structure at any level was not a minimum energy structure. Two imaginary frequencies of irreducible representation belong to A''. But if the molecule were C<sub>1</sub>, there would not be any relevant distribution whereas the molecule has a true minimum energy  $E(\text{B3LYP}) = -786.62535$  a.u. for C<sub>1</sub> symmetry and  $E(\text{B3LYP}) = -786.62120$  a.u. for C<sub>s</sub> symmetry by using 6-311++G(d,p). By using the same method and basis set, it was seen that all the vibrational frequencies were positive. Therefore, we were confident that a definite absolute minimum energy in the potential surface was found. The C<sub>1</sub> symmetry structure was the lowest energy at all levels. All fundamental vibrations are active in both IR and Raman. We know that ab initio HF and DFT potentials systematically overestimate the vibrational wavenumbers. These discrepancies are corrected either by computing anharmonic cor-

**Table 2**  
Comparison calculated and experimental (FT-IR and FT-Raman) vibrational spectra and related assignments of 4-chloro-N-methylaniline.

No.	Experimental		B3LYP				TED ( $\geq 10\%$ )
	IR	Ra	Scaled	$I_{IR}$	$S_{Ra}$	$I_{Ra}$	
1		82 vs	80	1.97	0.41	74.23	$\gamma(\text{ring-NHCH}_3)$ (57) + $\gamma\text{CCl}$ (12)
2			134	0.54	0.23	17.17	$\tau(\text{ring-NHCH}_3)$ (78)
3		186 w	182	2.12	1.96	88.25	$r(\text{ring-NHCH}_3)$ (63) + $\beta\text{CCl}$ (19)
4			209	0.30	1.26	46.31	$\tau\text{CH}_3$ (85)
5		294 w	285	21.04	3.27	75.52	$\beta\text{CCl}$ (43) + $\beta\text{C-N-CH}_3$ (33) + $\gamma\text{NH}$ (11)
6			315	1.68	0.42	8.4	$\gamma\text{Cl-ring-N}$ (72)
7			359	2.56	7.08	118	$\beta\text{CCC}$ (33) + $\nu\text{CCl}$ (27) + $\beta\text{CCCl}$ (13) + $\beta\text{CCN}$ (12)
8		366 s	371	108.06	2.53	40.42	$\gamma\text{NH}$ (77)
9	412 w		417	0.18	0.09	1.22	$\gamma(\text{CH})_{\text{ring}}$ (99)
10	507 w		506	15.36	0.55	5.76	$\gamma\text{CCC}$ (72)
11			511	38.05	0.65	6.73	$\beta\text{CNC}$ (21) + $\gamma\text{NH}$ (19) + $\nu\text{CCl}$ (13)
12		628 w	632	4.57	3.09	24.08	$\beta\text{CCC}$ (77)
13	641w		647	15.79	4.56	34.45	$\beta\text{CCC}$ (55) + $\nu\text{CCl}$ (19)
14	698 w		709	2.11	0.10	0.66	$\gamma\text{CCC}$ (51) + $\gamma\text{CH}$ (27)
15			793	0.15	0.38	2.17	$\gamma(\text{CH})_{\text{ring}}$ (97)
16		805 s	804	3.53	28.97	162.69	$\beta\text{CCC}$ (46) + $\nu\text{CN}$ (15)
17	816 s		812	61.94	1.09	6.02	$\gamma(\text{CH})_{\text{ring}}$ (71)
18	925 w		923	0.46	0.04	0.184	$\gamma(\text{CH})_{\text{ring}}$ (80)
19			939	0.01	0.11	0.49	$\gamma(\text{CH})_{\text{ring}}$ (88)
20	1002 w	996w	999	7.70	3.93	16.11	$\beta\text{CCC}$ (85)
21	1060w	1056 w	1056	11.85	15.01	56.16	$\nu\text{N-CH}_3$ (50) + $\nu\text{CC}$ (16) + $\nu\text{r-CH}_3$ (14)
22	1093m	1095 s	1086	35.54	24.21	87.43	$\nu\text{CC}$ (43) + $\nu\text{CCl}$ (16)
23			1107	4.67	0.65	2.28	$\beta(\text{CH})_{\text{ring}}$ (41) + $\nu\text{CC}$ (22) + $\text{rN-CH}_3$ (10)
24	1117m	1118 m	1126	9.83	1.82	6.22	$\rho\text{CH}_3$ (95)
25	1155 ms		1158	10.82	1.26	4.11	$\text{rN-CH}_3$ (56) + $\nu\text{N-CH}_3$ (14)
26	1178 w	1177 w	1182	21.85	7.03	22.23	$\beta(\text{CH})_{\text{ring}}$ (75) + $\nu\text{CC}$ (19)
27	1260 ms		1269	53.17	3.05	8.607	$\nu\text{CC}$ (43) + $\nu\text{CN}$ (27) + $\beta\text{NH}$ (10)
28	1295 ms	1295 w	1300	3.80	2.49	6.74	$\beta(\text{CH})_{\text{ring}}$ (71) + $\nu\text{CC}$ (23)
29	1318 m		1320	78.74	11.58	30.61	$\nu\text{CC}$ (42) + $\nu\text{CN}$ (23) + $\beta(\text{CH})_{\text{ring}}$ (10)
30	1395 w		1401	8.05	1.07	2.55	$\nu\text{CC}$ (35) + $\beta(\text{CH})_{\text{ring}}$ (25)
31	1431m	1430 w	1443	5.69	6.16	13.99	$\omega\text{CH}_3$ (91)
32	1448 s		1461	13.84	14.50	32.21	$\rho\text{CH}_2$ (86)
33	1469 w		1480	9.83	2.83	6.155	$\rho\text{CH}_2$ (37) + $\beta\text{NH}$ (27)
34	1504 w		1498	6.30	7.46	15.88	$\rho\text{CH}_2$ (57)
35			1512	261.65	2.48	5.18	$\beta\text{NH}$ (20) + $\nu(\text{CC})$ (17) + $\beta(\text{CH})_{\text{ring}}$ (16) + $\nu\text{CN}$ (13)
36			1588	1.72	2.42	4.62	$\nu_{\text{asym}}(\text{CCC})$ (65) + $\beta\text{NH}$ (11)
37	1604 s	1600 s	1615	81.04	76.27	141.59	$\nu\text{C}=\text{C}$ (80)
	1734 w					100	Overtone/combination
	1866 w					44.69	Overtone/combination
	2360 w					48.52	Overtone/combination
	2576 w					35.23	Overtone/combination
	2814 w	2809 vw				19.24	Overtone/combination
38	2886 m		2851	84.01	217.11	34.96	$\nu(\text{CH})_{\text{methyl}}$ (100)
39	2930 w		2923	34.71	99.72	55.23	$\nu(\text{CH})_{\text{methyl}}$ (100)
40	2986 w	2980 w	2983	20.98	114.89	29.42	$\nu(\text{CH})_{\text{methyl}}$ (96)
41	3022 w		3025	13.62	87.02	74.23	$\nu(\text{CH})_{\text{ring}}$ (100)
42	3054 w		3054	5.42	48.92	17.17	$\nu(\text{CH})_{\text{ring}}$ (100)
43		3067 s	3063	4.19	89.63	88.25	$\nu(\text{CH})_{\text{ring}}$ (98)
44			3069	4.98	142.41	46.31	$\nu(\text{CH})_{\text{ring}}$ (98)
45	3428 s		3474	25.84	114.09	75.52	$\nu\text{NH}$ (100)

Scalefactor: wavenumber in ranges from 4000 to 400  $\text{cm}^{-1}$  and lower than 1700  $\text{cm}^{-1}$  are scaled with 0.958 and 0.983 for B3LYP/6-311++G(d,p) basis set [43],  $I_{IR}$ —IR Intensity ( $\text{K mmol}^{-1}$ ),  $I_{Ram}$ —Raman intensity (Arb units),  $\nu$ —stretching;  $\beta$ —in-plane-bending;  $\gamma$ —out-of-plane bending;  $\omega$ —wagging;  $\rho$ —rocking;  $t$ —twisting;  $\tau$ —torsion.

rections explicitly or by introducing scaling factor for B3LYP with 6-311+G(d,p) basis set, the wavenumbers in the ranges from 4000 to 1700  $\text{cm}^{-1}$  and lower than 1700  $\text{cm}^{-1}$  are scaled with 0.958 and 0.983, respectively [43]. After scaling with a scaling factor, the deviation from the experiment is less than 10  $\text{cm}^{-1}$  with a few exceptions.

#### 4.2.1. C–H vibrations

The heteroaromatic structure show the presence of C–H stretching vibrations in the region 3100–3000  $\text{cm}^{-1}$  which is the characteristic region for the ready identification of C–H stretching vibrations [44]. In this region, the bands are not affected appreciably by the nature of substituents. The 4-CINMA has two adjacent aromatic C–H units on both sides of ring. The C2–H, C3–H, C5–H and C6–H stretching vibrations corresponds to mode nos. 44, 43,

42 and 41 in the region 3069–3025  $\text{cm}^{-1}$  by B3LYP method show excellent agreement with FT-IR spectrum at 3054, 3022  $\text{cm}^{-1}$  and 3067  $\text{cm}^{-1}$  in FT-Raman spectrum.

The aromatic C–H in-plane bending modes of benzene and its derivatives are observed in the region 1300–100  $\text{cm}^{-1}$  [44]. The bands are observed in the FT-IR spectrum at 1295 and 1178  $\text{cm}^{-1}$  and their counter part of the FT-Raman spectrum at 1295 and 1177  $\text{cm}^{-1}$  are assigned to C–H in-plane bending vibration. The theoretically computed B3LYP method at 1300, 1182 and 1107  $\text{cm}^{-1}$  (modes nos. 28, 26 and 23) show good agreement with recorded as well as literature data [34]. The bands observed at 925 and 816  $\text{cm}^{-1}$  in FT-IR spectrum are assigned to C–H out-of-plane bending vibrations for 4-CINMA. These also show good agreement with theoretically scaled harmonic wavenumber values at 939, 923, 812 and 793  $\text{cm}^{-1}$  by B3LYP method.

#### 4.2.2. Phenyl ring modes

The ring carbon–carbon stretching vibration occurs in the region 1625–1430  $\text{cm}^{-1}$ . In general, the bands are of variable intensity and observed at 1625–1590, 1590–1575, 1540–1470, 1460–1430 and 1380–1280  $\text{cm}^{-1}$  from the frequency ranges given by Varsanyi [44] for the five bands in the region. In the present work, the frequencies observed in the FT-IR spectrum at 1395, 1318 and 1260  $\text{cm}^{-1}$  are assigned to C–C stretching vibrations. The same vibrations in the FT-Raman spectrum are absent. The ring breathing mode at 1093  $\text{cm}^{-1}$  in FT-IR and the same vibration in FT-Raman at 1095  $\text{cm}^{-1}$  coincide exactly with B3LYP predicted value at 1086  $\text{cm}^{-1}$  (mode no. 22). The TED of this vibration is a mixed mode as it is evident from Table 2 mixed with C–Cl stretching mode. The in-plane deformations are at higher frequencies than those of out-of-plane vibrations. Shimanouchi et al. [45] gave the frequency data for this vibrations for different benzene derivatives as a result of normal coordinate analysis. The bands at 805, 698, 641, 628 and 507  $\text{cm}^{-1}$  in both FT-IR and FT-Raman spectra are assigned to C–C deformation of phenyl ring. The theoretically computed C–C–C out-of-plane and in-plane bending vibrational modes have been found to be consistent with recorded spectral value. The TED of these vibrations are not pure modes as it is evident from the last column of TED in Table 2.

#### 4.2.3. C–Cl vibrations

The vibrations belonging to the bond between the ring and halogen atoms are worth to discuss here since mixing of vibrations are possible due to the lowering of molecular symmetry and the presence of heavy atoms on periphery of the molecule [46,47]. The assignment of C–Cl stretching and deformation vibrations have been made by comparison with similar molecules, *p*-bromophenol [49] and the halogen substituted benzene derivatives [45]. Mooney [48,49] assigned vibrations of C–X group (X = Cl, Br, I) in the frequency range 1129–480  $\text{cm}^{-1}$ . The C–Cl stretching vibration gives, strong bands in the region 710–505  $\text{cm}^{-1}$ . Compounds with more than one chlorine atom exhibit very strong bands due to asymmetric and symmetric stretching modes. Vibrational coupling with other groups may result in a shift in the absorption to as high as 840  $\text{cm}^{-1}$ . For simple organic chlorine compounds, C–Cl absorptions are in the region 750–700  $\text{cm}^{-1}$ , whereas for the trans and gauche forms [49,50] they are near at 650  $\text{cm}^{-1}$ . In the FT-IR spectrum of our title molecule 4-CINMA at 641  $\text{cm}^{-1}$  is assigned to C–Cl stretching vibration. The theoretical calculation by B3LYP method at 647  $\text{cm}^{-1}$  exactly correlates with experimental observation. The TED of this vibration show strong mixing with C–C–C in-plane bending as shown in Table 2.

#### 4.2.4. Methyl group vibration

The molecule 4-chloro-N-methylaniline possesses one  $\text{CH}_3$  group. For the assignments of  $\text{CH}_3$  group frequency one can expect the nine fundamentals that can be associated to each  $\text{CH}_3$  group, namely the symmetrical stretching in  $\text{CH}_3$  ( $\text{CH}_3$  sym. stretching); the asymmetrical stretching ( $\text{CH}_3$  asym. stretching); the symmetrical ( $\text{CH}_3$  sym. deformation) and asymmetrical ( $\text{CH}_3$  asym. deformation) deformations modes; in-plane rocking ( $\text{CH}_3$  ipr), out-of-plane rocking ( $\text{CH}_3$  opr) and twisting ( $\text{tCH}_3$ ) bending modes.

The C–H stretching in  $\text{CH}_3$  group occurs at lower wavenumbers than those of aromatic ring (3000–3100  $\text{cm}^{-1}$ ). The symmetric C–H stretching mode of  $\text{CH}_3$  group is expected in the region around 2980  $\text{cm}^{-1}$  and symmetric [51–53] one is expected around the region 2810  $\text{cm}^{-1}$ . For 2-methylpyridine the  $\text{CH}_3$  stretching is around 1450–1370  $\text{cm}^{-1}$  and rocking 1020–980  $\text{cm}^{-1}$  [54]. In accordance with the above conclusion, the theoretically predicted asymmetric and symmetric stretching vibrations in  $\text{CH}_3$  is at 2983, 2923 and 2851  $\text{cm}^{-1}$  by B3LYP/6-311++G(d,p) method (mode nos. 40–38). The FT-IR band at 2986, 2930 and 2886 represents the asymmetric and symmetric stretching vibrations are exactly correlated

with theoretical data. The counterpart in FT-Raman at 2980  $\text{cm}^{-1}$  corresponds to asymmetric stretching in  $\text{CH}_3$  group. As expected these three modes are pure stretching modes as it is evident from TED column, they are almost contributing to 100%.

For the methyl substituted benzene derivatives the asymmetric and symmetric deformation vibrations of methyl group normally appear in the region 1465–1440 and 1390–1370  $\text{cm}^{-1}$ , respectively [54,55]. The wavenumbers of the modes involving the  $\text{CH}_3$  deformation vibration agree with the commonly accepted region of these vibrations [56,57]. The work carried by Long and Joergel [58] on 4-methylpyridine, the frequency of 1041 and 974  $\text{cm}^{-1}$  in FT-Raman are assigned to the rocking modes of  $\text{CH}_3$ . The rocking vibrations of the  $\text{CH}_3$  group in 4-CINMA appear as independent vibrations. These modes usually appear [54] in the region 1070–1020  $\text{cm}^{-1}$ . The weak band in FT-IR at 1117 and a weak band at 1118  $\text{cm}^{-1}$  in FT-Raman are attributed to the  $\text{CH}_3$  rocking mode. The theoretical value by B3LYP/6-311++G(d,p) method at 1126  $\text{cm}^{-1}$  (mode no. 24) shows excellent agreement with the experimental observation. As expected the  $\text{CH}_3$  torsional mode appear below 400  $\text{cm}^{-1}$ , the computed band at 209  $\text{cm}^{-1}$  by B3LYP method show excellent correlation with literature data, however for the same mode, the experimental bands are absent due to overcrowding of low frequency vibration. The TED for this vibration is almost contributing to 85% as shown in Table 2.

#### 4.2.5. N–H vibration

The heteroaromatic structure shows the presence of C–H and N–H stretching vibrations above 3000  $\text{cm}^{-1}$  which is the characteristic region for ready identification of this structure [59,60]. These are usual ranges for  $\text{CH}_3$ ,  $\text{NH}_2$  and C–H vibrations. The N–H stretching vibrations occur in the region 3200–3500  $\text{cm}^{-1}$ . The scaled N–H stretch is calculated at 3474  $\text{cm}^{-1}$  and the experimental value observed at 3428  $\text{cm}^{-1}$  in FT-IR. The TED of these vibrations is exactly contributing to 100% as shown in last column of Table 2. The N– $\text{CH}_3$  stretching vibration is calculated at 1056  $\text{cm}^{-1}$ . This vibration also shows exact correlation with experimental observation at 1060  $\text{cm}^{-1}$  in FT-IR and 1056  $\text{cm}^{-1}$  in FT-Raman spectrum.

#### 4.2.6. C–N stretching vibration

The C–N stretching frequency is a rather difficult task since there are problems in identifying these frequencies from other vibrations. Silverstein et al. [59] identified the C–N stretching absorption in the region 1382–1266  $\text{cm}^{-1}$  for aromatic amines. The C–N stretching is observed at 1293  $\text{cm}^{-1}$  [61]. Hence the band at 1260  $\text{cm}^{-1}$  in FT-IR spectrum is assigned to C–N stretching vibration. The theoretically predicted scaled value at 1269  $\text{cm}^{-1}$  (mode no. 27) show excellent agreement with experimental data. The TED of this vibration suggests that this is a mixed mode with C–C stretching vibration. It has also some contribution in the mode no. 29.

#### 4.2.7. NMR spectra

The isotropic chemical shifts are frequently used as an aid in identification of relative ionic species. It is recognized that accurate predictions of molecular geometries are essential for reliable calculations of magnetic properties. The experimental and calculated values for  $^{13}\text{C}$  and  $^1\text{H}$  NMR are shown in Table 3. As in Fig. 6, the studied molecule shows seven different carbon atoms. Taking into account that the range of  $^{13}\text{C}$  NMR chemical shift for analogous organic molecules usually is >100 ppm [62,63], the accuracy ensures reliable interpretation of spectroscopic parameters. In the present work,  $^{13}\text{C}$  NMR chemical shifts in the ring for the title molecule are >100 ppm, as they would be expected (in Table 3). Nitrogen atom shows electronegative property. Therefore, the chemical shift value of C4 which is in the ring has been observed at 145.7 ppm. C–N calculated (with respect to TMS) 155.2 ppm. Similarly, five carbon peaks in the ring are observed from 113.63 to

**Table 3**

The experimental and predicted  $^{13}\text{C}$  and  $^1\text{H}$  isotropic chemical shifts (with respect to TMS, all values in ppm) for 4-CINMA.

Atom	Exp.	B3LYP	Atom	Exp.	B3LYP
C(1)	122.70	132.91	H(7)	6.524	7.30
C(2)	129.22	133.63	H(8)	7.148	6.64
C(3)	113.63	119.34	H(10)	3.618	4.13
C(4)	145.70	155.19	H(12)	2.889	2.85
C(5)	113.63	112.54	H(13)	2.736	2.57
C(6)	129.22	134.34	H(14)	2.886	2.83
C(11)	29.70	30.41	H(15)	6.516	7.43
			H(17)	7.141	6.82

129.2 ppm are calculated from 112.54 to 134.34 ppm. Moreover, the pairs C3/C5 as well as C2/C6 are expected to be isochronous due to signal averaging, and only two signals for the C–H carbons are expected. This results also support our theoretical results as shown in Table 3. Besides, another carbon peak is calculated at 31.41 ppm, that is observed at 29.70 ppm (N–CH<sub>3</sub>).

The studied molecule has four hydrogen atoms in the ring, three hydrogen atoms attached to the carbon atom of methyl group and one hydrogen attached in the nitrogen atom. In the  $^1\text{H}$  NMR spectra just one type of protons appears at 2.80 ppm as a singlet (CH<sub>3</sub>), where as the chemical shift value (with respect to TMS) of 2.85, 2.74 and 2.83 ppm have been determined by using B3LYP/6-311++G(d,p) method, the values are listed in Table 3. The remainder of the observed and calculated  $^1\text{H}$  NMR isotropic chemical shift value are listed in Table 3. As can be seen from Table 3, there is a very good agreement between experimental and theoretical chemical shift results for the title molecule. The signal at 1.56 ppm is due to H<sub>2</sub>O in CDCl<sub>3</sub>.

## 5. Conclusion

The optimized molecular structures, vibrational frequencies and corresponding vibrational assignments of 4-CINMA have been calculated using B3LYP/6-311++G(d,p) method. Comparison of the experimental and calculated spectra of the molecule showed that DFT-B3LYP method is in good agreement with experimental data. On the basis of agreement between the calculated and observed results, assignments of fundamental vibrational modes of 4-CINMA were examined and some assignments were proposed. This study demonstrates that scaled DFT/B3LYP calculations are powerful approach for understanding the vibrational spectra of medium sized organic compounds.  $^1\text{H}$  and  $^{13}\text{C}$  NMR chemical shifts have been compared with experimental values.

## Acknowledgements

The visit of Dr. N. Sundaraganesan, to Ahi Evran University was facilitated by Scientific and Technological Research Council of TURKEY (TUBİTAK) BİDEB-2221.

## References

- [1] A. Altun, K. Gölcük, M. Kumru, *J. Mol. Struct. (Theochem.)* 625 (2003) 17.
- [2] J. Whysner, L. Vera, G.M. Williams, *Pharmacol. Ther.* 71 (1996) 107.
- [3] E. Akalin, S. Akyüz, *J. Mol. Struct.* 571 (2003) 651.
- [4] A. Malinuaskas, R. Garjonytė, R. Mažeikienė, I. Jurevičiūtė, *Talanta* 64 (2004) 121.
- [5] M.N. Nadagouda, R. Rajender, S. Varma, *Macromol. Rapid Commun.* 28 (2007) 2106.
- [6] W.B. Tzeng, K. Narayanan, *J. Mol. Struct. (Theochem.)* 434 (1998) 247.
- [7] R. Mažeikienė, G. Niaura, A. Malinuaskas, *J. Solid State Electrochem.* 11 (2007) 923.
- [8] M. Fujitake, J. Aoyama, N. Ohashi, *J. Mol. Spectrosc.* 235 (2006) 27.
- [9] Ş. Yurdakul, A.I. Sen, *Vib. Spectrosc.* 20 (1999) 27.
- [10] B. Ballesteros, E. Marinez, L. Sontos, J. Sanchez-Marin, *J. Mol. Struct.* 605 (2002) 225.
- [11] W.B. Tzeng, K. Narayanan, J.L. Lin, C.C. Tung, *Spectrochim. Acta* 55A (1999) 153.
- [12] M. Castellá-Ventura, E. Kassab, *Spectrochim. Acta* 50A (1994) 69.
- [13] A.D. Gorse, M. Pesquer, *J. Mol. Struct. (Theochem.)* 281 (1993) 21.
- [14] C.W. Bock, P. George, M. Trachtman, *Theor. Chim. Acta* 69 (1986) 235.
- [15] Y. Wang, S. Saebø, C.U. Pittman, *J. Mol. Struct. (Theochem.)* 281 (1993) 91.
- [16] J.C. Evans, *Spectrochim. Acta* 16 (1960) 428.
- [17] G.D. Lister, J.K. Tyler, J.H. Hog, N.W. Larsen, *J. Mol. Struct.* 23 (1974) 253.
- [18] M. Fukuyo, K. Hirotsu, T. Higuchi, *Acta Crystallogr.* 38B (1982) 640.
- [19] J. Reuben, *J. Am. Chem. Soc.* 109 (2) (1987) 316.
- [20] E. Akalin, S. Akyüz, *J. Mol. Struct.* 482 (1999) 175.
- [21] I. López-Tocón, M. Becucci, G. Pietraperzia, E. Castelluchi, J.C. Otero, *J. Mol. Struct.* 556 (2001) 421.
- [22] M.E. Vaschetto, B.A. Retamal, A.P. Monkman, *J. Mol. Struct. (Theochem.)* 468 (1999) 209.
- [23] C. Engelter, D.A. Thornton, M.R. Ziman, *J. Mol. Struct.* 49 (1978) 7.
- [24] C. Engelter, D.A. Thornton, M.R. Ziman, *J. Mol. Struct.* 33 (1976) 119.
- [25] G. Varsanyi, *Assignments of Vibrational Spectra of 700 Benzene Derivatives*, Wiley, New York, 1974.
- [26] A. Altun, K. Gölcük, M. Kumru, *J. Mol. Struct. (Theochem.)* 637 (2003) 155.
- [27] N. Sundaraganesan, H. Saleem, S. Mohan, M. Ramalingam, *Spectrochim. Acta* 61A (2005) 377.
- [28] S.N. Sharma, C.P.D. Dwivedi, *Indian J. Pure Appl. Phys.* 13 (1975) 570.
- [29] R. Shanker, R.A. Yadav, I.S. Singh, O.N. Singh, *Indian J. Pure Appl. Phys.* 23 (1985) 339.
- [30] J. Barluenga, F.J. Fananas, R. Sanz, Y. Fernandez, *Chem. Eur. J.* 9 (2002) 8.
- [31] L. Lunazzi, C. Magagnoli, M. Guerra, D. Macciantelli, *Tetrahedron Lett.* 20 (1979) 3031.
- [32] B.K. Barr, A.J. Herman, L.K. Myers, P.I. Young, C.D. Schaeffer Jr., H.J. Eppley, J.C. Otter, H. Yoder, *J. Organomet. Chem.* 434 (1992) 45.
- [33] P.C. Stein, W.L. Earl, A. Ray, *Synth. Met.* 55 (1993) 702.
- [34] M. Karabacak, M. Kurt, M. Cinar, A. Coruh, *Mol. Phys.* 107 (2009) 253.
- [35] M. Karabacak, M. Kurt, A. Atac, *J. Phys. Org. Chem.* 22 (2009) 321.
- [36] Gaussian 03 Program, Gaussian Inc., Wallingford, CT, 2004.
- [37] H.B. Schlegel, *J. Comput. Chem.* 3 (1982) 214.
- [38] K. Wolinski, J.F. Hinton, P. Pulay, *J. Am. Chem. Soc.* 112 (1990) 8251.
- [39] J. Baker, A.A. Jarzocki, P. Pulay, *J. Phys. Chem.* 102A (1998) 1412.
- [40] G. Keresztury, S. Holly, J. Varga, G. Besenyei, A.Y. Wang, J.R. Durig, *Spectrochim. Acta* 49A (1993) 2007.
- [41] Raman spectroscopy: theory, in: G. Keresztury, J.M. Chalmers, P.R. Griffith (Eds.), *Hand book of Vibrational Spectroscopy*, vol. 1, John Wiley & Sons Ltd., New York, 2002.
- [42] J.H. Palm, *Acta Crystallogr.* 21 (1966) 473.
- [43] N. Sundaraganesan, S. Illakiamani, H. Saleem, P.M. Wojciechowski, D. Michalska, *Spectrochim. Acta* 61A (2005) 2995.
- [44] G. Varsanyi, *Assignment for Vibrational Spectra of Seven Hundred Benzene Derivatives*, vols. 1–2, Adam Hilger, 1974.
- [45] T. Shimanouchi, Y. Kakiuti, I. Gamo, *J. Chem. Phys.* 25 (1956) 1245.
- [46] C. Lee, W. Yang, R.G. Parr, *Phys. Rev.* 37B (1988) 785.
- [47] M. Bakiler, I.V. Maslov, S. Akyüz, *J. Mol. Struct.* 475 (1999) 83.
- [48] E.F. Mooney, *Spectrochim. Acta* 20 (1964) 1021.
- [49] E.F. Mooney, *Spectrochim. Acta* 19 (1964) 877.
- [50] G. Socrates, *Infrared Characteristic Group Frequencies*, John Wiley, New York, 2000.
- [51] G. Varsanyi, *Vibrational Spectra of Benzene Derivatives*, Academic Press, New York, 1969.
- [52] D.A. Kleinman, *Phys. Rev.* 126 (1962) 1977.
- [53] B. Smith, *Infrared Spectral Interpretation: A Systematic Approach*, CRC Press, Washington, DC, 1999.
- [54] N. Sundaraganesan, S. Illakiamani, B.D. Joshua, *Spectrochim. Acta* 67A (2007) 287.
- [55] M.A. Palafox, M. Gil, J.L. Nunez, *Vib. Spectrosc.* 6 (1993) 95.
- [56] N.B. Colthup, L.H. Daly, S.E. Wiberly, *Introduction to Infrared and Raman Spectroscopy*, Academic Press, New York, 1990.
- [57] J.F. Areanas, I. Lopez Tocn, J.C. Otero, J.I. Marcos, *J. Mol. Struct.* 433 (1997) 410.
- [58] D.A. Long, W.O. Joerge, *Spectrochim. Acta* 19 (1963) 1777.
- [59] M. Silverstein, G. Clayton Basseler, C. Morill, *Spectrometric Identification of Organic Compounds*, Wiley, New York, 1981.
- [60] V. Krishnakumar, P. Ramasamy, *Spectrochim. Acta* 62A (2005) 570.
- [61] C. Engelter, D.A. Thornton, M.R. Ziman, *J. Mol. Struct.* 49 (1978) 7.
- [62] H.O. Kalinowski, S. Berger, S. Braun, *Carbon-13 NMR spectroscopy*, John Wiley and Sons, Chichester, 1988.
- [63] K. Pihlaja, E. Kleinpeter, *Carbon-13 Chemical Shifts in Structural and Stereo Chemical Analysis*, VCH Publishers, Deerfield Beach, 1994.